

# Assessment of Diabetic Foot Wound by using Wound Boundary Determination and Analysis Algorithm

[1] S.Anandhajothi, [2] M.Jeyalakshmi, [3] B.Shanmathi, [4] Manimegalai

[1] [2] [3] UG Student, [4] Assistant Professor P.S.R.Rengasamy College of Engineering for Women, Sivakasi

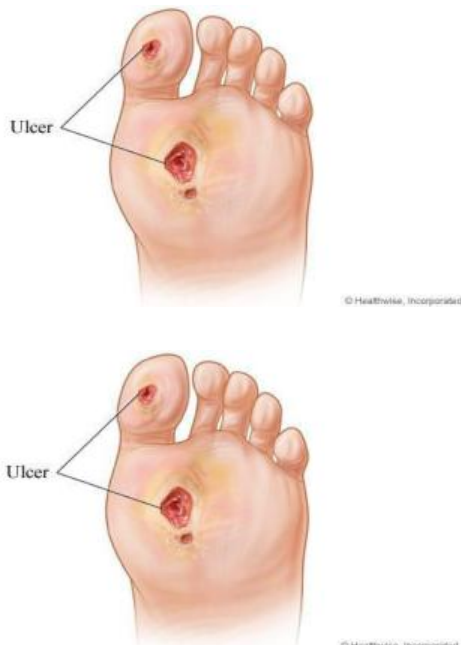
[1] [baskaransathyavathy@gmail.com](mailto:baskaransathyavathy@gmail.com), [4] [mm11.1990@gmail.com](mailto:mm11.1990@gmail.com)

**Abstract:** A diabetic foot ulcer is an open sore or wound that occurs in approximately 15 percent of patients with diabetes and is commonly located on the bottom of the foot. Diabetic patients can check their wound healing by sitting in the house itself, this can save travel cost and reduce healthcare expenses. In this paper, we propose a wound image analysis by using mean shift algorithm. First, the diabetic wound picture is captured by the camera. After that, the wound image is segmented by using mean shift algorithm. Especially, the outline of the foot is determined based on skin colour and also boundary of the wound is found. Within the foot, the wounded area is coloured by RGB (red-green-black). Apart from that wounded area is to be normal skin colour. Our system can be effectively used to analyze the wound healing status approximately.

**Index Terms**— Patients with diabetes, Wound Analysis, Mean shift, Camera.

## I. INTRODUCTION

Diabetes refers to a condition in which the body is not using efficiently the glucose and its found in large amount in the blood. Major affective part of the diabetes is diabetic foot. The development of the foot ulcer starts with lower limb generating high pressure and skin infection. Foot ulcers are a common complication of poorly controlled diabetes. A diabetic foot ulcer is an open wound which is located on the bottom of the foot.



There are many problems with current practices for treating diabetic foot ulcers. First, patients must go to their wound clinic on a regular basis to have their wounds checked by their clinicians. This need for frequent clinical evaluation is not only inconvenient and time consuming for patients and clinicians, but also represents a significant health care cost because patients may require special transportation. Second, a clinician's wound assessment process is based on visual examination. He/she describes the wound by its physical dimensions and the color of its tissues, providing important indications of the wound type and the stage of healing. Because the visual assessment does not produce objective measurements and quantifiable parameters of the healing status [7], tracking a wound's healing process across consecutive visits is a difficult task for both clinicians and patients.

Technology employing image analysis techniques is a potential solution to both these problems. Several attempts have been made to use image processing techniques for such tasks, including the measurement of area, or alternatively using a volume instrument system (MAVIS) or a medical digital photogrammetric system (MEDPHOS). These approaches suffer from several drawbacks including high cost, complexity and lack of tissue classification.

To better determine the wound boundary and classify wound tissues, researchers have applied image segmentation and supervised machine learning algorithm for wound analysis. A French research group proposed a method of using a support vector machine (SVM) based wound classification method. The same idea has also been employed in for the detection of melanoma at a curable stage. Although the SVM classifier method led to good results on typical wound images [10], it is not feasible to implement the training process and the feature extraction on current cameras due to its computational demands. Furthermore, the supervised learning algorithm requires a large number of training image samples and experienced clinical input, which is difficult and costly.

Our solution provides image analysis algorithms that run on a camera, and thus provide a low cost and easy-to-use device for self-management of foot ulcers for patients with type 2 diabetes. Our solution engages patients as active participants in their own care, meeting the recommendation of the Committee on Quality of Health Care in America to provide more information technology (IT) solutions. The solution

widely used commodity camera containing a high-resolution camera is a viable candidate for image capture and image processing provided that the processing algorithms are both accurate and well-suited for the available hardware and computational resources. To convert an ordinary camera into a practical device for self-management of diabetic wounds, we need to address two tasks: (i) Develop a simple method for patients to capture an image of their foot ulcers. (ii) Design a highly efficient and accurate algorithm for real-time wound analysis that is able to operate within the computational constraints of the camera.

Our solution for task (i) was specifically designed to aid patients with type 2 diabetes in photographing ulcers occurring on the sole of their feet. This is particularly challenging due to mobility limitations, common for individuals with advanced diabetes. To this end, we designed and built an image capture box with an optical system containing a dual set of front surface mirrors, integrated LED lighting and a comfortable, slanted surface for the patients to place their foot. The design ensures consistent illumination and a fixed optical path length between the sole of the foot and the camera, so that pictures captured at different times would be taken from the same camera angles and under the same lighting conditions. Task (ii) was implemented by utilizing an accurate, yet computationally efficient algorithm, *i.e.*, the mean shift algorithm, for wound boundary determination, followed by color segmentation within the wound area for assessing healing status.

The wound boundary determination was done with a particular implementation of the level set algorithm, specifically the *distance regularized level set evolution* (DRLSE). The principal disadvantage of the level set algorithm is that the iteration of global level set function is too computationally intensive to be implemented on cameras, even with the narrow band confined implementation based on GPUs. The level set evolution completely depends on the initial curve which has to be pure-delineated either manually or by a well-designed algorithm.

To address these problems, The level set algorithms with the efficient mean shift segmentation algorithm. It also creates additional challenges, such as over-segmentation. It present the entire process of recording and examine a wound image, that are executable on a camera, and provide proof of the planning and accuracy for inspect diabetic foot ulcers.

Section II-A provides an overview of the structure of the wound image analysis software system. Section II-B briefly introduces the mean shift algorithm used in our system and related region merge methods. Section II-C introduces the wound analysis method. This is based on the image segmentation results including foot outline detection, wound boundary determination, color segmentation within the wound and healing status evaluation. In Section III, the GPU optimization method of the mean shift segmentation algorithm is discussed. Section IV presents the image capture box designed for patients with diabetic foot ulcers to easily use the camera to take an image of the bottom of their foot. Experimental results are presented and analyzed in Section V. Finally, Section VI provides an overall assessment of the wound image analysis system.

## II. WOUND ANALYSIS METHOD

### A. Wound Image Analysis System Overview

Our quantitative wound assessment system consists of several functional modules including wound image capture, wound image storage, wound image segmentation, foot outline detection, wound boundary determination, wound analysis by color segmentation. All these processing steps are carried out solely by the computational resources of the camera. The functional diagram of our quantitative wound assessment system is shown as in Figure 1 and explained below. All these processing steps are carried out solely by the computational resources of the camera. Note that the words highlighted in bold in the text correspond to specific blocks in figures with block diagrams. While the image capture is the first step in the flow chart, the image capture box is not one of the image processing steps and is therefore presented later in Section IV.

A camera was chosen due to its excellent performance and high resolution camera. Although there are likely performance variations across the modern cameras, such a study was considered beyond the scope of this paper. After the wound image is captured, the JPEG file path of this image is added into a wound image database. This compressed image file, which cannot be processed directly with our main image processing algorithms, therefore needs to be decompressed into a 24-bit bitmap file based on the standard RGB color model. In our system, we use camera to accomplish the JPEG compression and decompression task. The “image quality” parameter was used to control the JPEG compression rate.

Setting “image quality” to 80 was shown empirically to provide the best balance between quality and storage space. For an efficient implementation on the camera alone, no method was used to further remove the artifacts introduced by JPEG lossy compression.

In the **Image preprocessing** step, we first down-sample the high resolution bitmap image to speed up the subsequent image analysis and to eliminate excessive details that may complicate wound image segmentation. In our case, we down-sample the original image (pixel dimensions 3264 x 2448) by a factor 4 in both the horizontal and vertical directions to pixel dimensions of 816 x 612, which has proven to provide a good balance between the wound resolution and the processing efficiency. In practice, we use the standard quality for image captured on the camera to ensure high efficiency. Second, we smooth the images to remove noise (assumed mainly to be Gaussian noise produced by image acquisition process) by using the Gaussian blur method whose standard deviation  $\sigma = 0.5$  was empirically judged to be optimal based on multiple experiments. To determine the boundary of the wound area, we first determine an outline of the foot within the image.

Hence the initial **Image segmentation** operation is to divide the original image into pixel groups with homogeneous color values. Specifically, the **Foot outline detection** is performed by finding the largest connected component in the segmented image under the condition that the color of this component is similar enough to a preset standard skin color. Based on the standard color checkers provided, both the light and dark skin color thresholds in CIE LAB space are incorporated into the system, which means that our algorithm is expected to work for most skin colors. Afterwards, we carry out a **Wound boundary determination** based on the foot outline detection result. If the foot detection result is regarded as a binary image with the foot area marked as “white” and rest part marked as “black”, it is easy to locate the wound boundary within the foot region boundary by detecting the largest connected “black” component within the “white” part. If the wound is located at the foot region boundary then the foot boundary is

not closed, and hence the problem becomes more complicated, i.e., we might need to first form a closed boundary.

When the wound boundary has been successfully determined and the wound area calculated, we next evaluate the healing state of the wound by performing **Color segmentation**, with the goal of categorizing each pixel in the wound boundary into certain classes labeled as granulation, slough and necrosis. The classical self-organized clustering method called K-mean with high computational efficiency is used [22]. After the color segmentation, a feature vector including the wound area size and dimensions for different types of wound tissues is formed to describe the wound quantitatively. This feature vector, along with both the original and analyzed images, is saved in the result database.

### B. Mean Shift Based Segmentation Algorithm

We chose the mean shift algorithm, proposed in [16], over other segmentation methods, such as level set and graph cut based algorithms, for several reasons. First, the mean shift algorithm takes into consideration the spatial continuity inside the image by expanding the original 3D color range space to 5D space, including two spatial components, since direct classification on the pixels proved to be inefficient [16]. Secondly, a number of acceleration algorithms are available. Thirdly, for both mean shift filtering and region merge methods, the quality of the segmentation is easily controlled by the spatial and color range resolution parameters [16] [17]. Hence, the segmentation algorithm can be adjustable to different degrees of skin color smoothness by changing the resolution parameters. Finally, the mean shift filtering algorithm is suitable for parallel implementation since the basic processing unit is the pixel. In this case, the high computational efficiency of GPUs can be exploited.

The mean shift algorithm belongs to the density estimation based non-parametric clustering methods, in which the feature space can be considered as the empirical probability density function of the represented parameter. This type of algorithms adequately analyzes the image feature space (color space, spatial space or the combination of the two spaces) to cluster and can provide a reliable solution for many vision tasks [16]. In general, the mean shift algorithm models the feature vectors associated with each pixel (e.g., color and position in the image grid) as samples from an unknown probability density function  $f(x)$  and then finds clusters in this distribution. The center for each cluster is called the mode [25]. Given  $n$  data points  $x_i, i=1, \dots, n$  in the  $d$ -dimensional space  $R^d$ , the multivariate kernel density estimator.

$$f_{h,K}(x) = \frac{c}{nh^d} \sum_{i=1}^n k\left(\frac{\|x - x_i\|}{h}\right) \quad (1)$$

where  $h$  is a bandwidth parameter satisfying  $h > 0$  and  $c_{k,d}$  is a normalization constant [16]. The function  $k(x)$  is the profile of the kernel defined only for  $x \geq 0$  and  $\|\cdot\|$  represents the vector norm. In applying the mean shift algorithm we use a variant of what is known in the optimization literature as multiple restart gradient descent. Starting at some guess at a local maximum  $y_k$ , which can be a random input data point  $x_i$ , the mean shift computes the density estimate  $f(x)$  at  $y_k$  and takes an uphill step using the gradient descent method. The gradient of  $f(x)$  is given as below.

$$f(x) = \frac{2c}{nh^d} \sum_{i=1}^n g\left(\frac{\|x - x_i\|}{h}\right) m(x) \quad (2)$$

$$m(x) = \frac{\sum_{i=1}^n \frac{x - x_i}{\|x - x_i\|} k\left(\frac{\|x - x_i\|}{h}\right)}{\sum_{i=1}^n k\left(\frac{\|x - x_i\|}{h}\right)} \quad (3)$$

where  $g(r) = k'(r)$  and  $n$  is the number of neighbors taken into account in the 5 dimension sample domain. In our case, we use the Epanechnikov kernel [26], which makes the derivative of this kernel a unit sphere. Based on [16], we use the combined kernel function shown in eq. (5) where  $h_s$  and  $h_r$  are different bandwidth values for spatial domain and range domain, respectively. In [16], the two bandwidth values are referred to as spatial and range resolutions. The vector  $m(x)$  defined in eq. (3) is called the mean shift vector [16], since it is the difference between the current value  $x$  and the weighted mean of the neighbors  $x_i$  around  $x$ . In the mean-shift procedure, the current estimate of the mode  $y_k$  at iteration  $k$  is replaced by its locally weighted mean as shown below in eq. (4) [16].

$$y_{k+1} = y_k + \frac{c}{h_s^2 h_r^3} \frac{m(y_k)}{k\left(\frac{\|x - y_k\|}{h_s}\right) k\left(\frac{\|x - y_k\|}{h_r}\right)} \quad (4)$$

$$K_{h_s, h_r}(x) = \frac{c}{h_s^2 h_r^3} k\left(\frac{\|x - y_k\|}{h_s}\right) k\left(\frac{\|x - y_k\|}{h_r}\right) \quad (5)$$

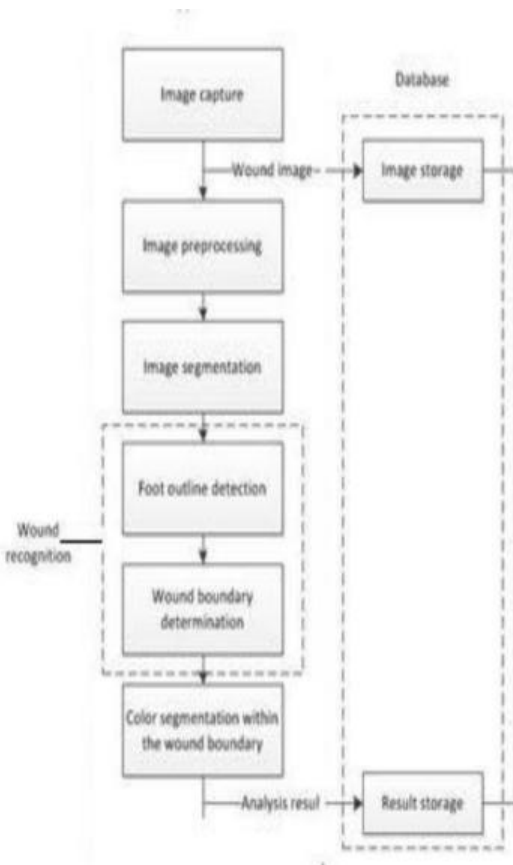


Fig. 1. Wound image analysis system software system

This iterative update of the local maxima estimation will be continued until the convergence condition is met. In our case, the convergence condition is specified as the Euclidean length of the mean shift vector that is smaller than a preset threshold. The threshold value for the mean shift iteration is the same for the task of locating the foot in the full image and for locating the wound within the foot boundary.

After the filtering (also referred to as the mode seeking) procedure above, the image is usually over-segmented, which means that there are more regions in the segmentation result than necessary for wound boundary determination [27]. To solve this problem, we have to merge the over-segmented image into a smaller number of regions which are more object-representative based on some rules. In the fusion step, extensive use was made of region adjacency graphs (RAG) [17] [28]. The initial RAG was built from the initial over-segmented image, the nodes being the vertices of the graph and the edges were defined based on 4-connectivity on the lattice.

The fusion was performed as a transitive closure operation [29] on the graph, under the condition that the color difference between two adjacent nodes should not exceed  $h_f$ , which is regarded as the region fusion resolution. The mean shift filtering and region fusion results of a sample foot wound image (part (a) in Figure 2) are shown in part (b) and (c) in Figure 2, respectively. We can see that the over-segmentation problem in part (b) is effectively solved by region fusion procedure. From the region fusion result in part (c), the foot boundary is readily determined by a largest connected component detection algorithm, which will be introduced in the next Section. A C++ based implementation method of the mean shift algorithm can be found.

### C. Wound Boundary Determination and Analysis Algorithms

Because the mean shift algorithm only manages to segment the original image into homogeneous regions with similar color features, an object recognition method is needed to interpret the segmentation result into a meaningful wound boundary determination that can be easily understood by the users of the wound analysis system. As noted in [30], a standard recognition method relies on known model information to develop a hypothesis, based on which a decision is made whether a region should be regarded as a candidate object, *i.e.*, a wound. A verification step is also needed for further confirmation. Because our wound determination algorithm is designed for real time implementation on the cameras with limited computational resources, we simplify the object recognition process while ensuring that recognition accuracy is acceptable.

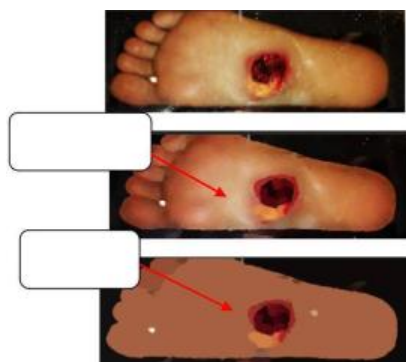


Fig. 2. Mean shift based image segmentation sample result. (a) Original image. (b) Mean shift filtered image. (c) Region fused image. Note that we artificially increased the brightness and contrast of the images in this figure to highlight the over-segmentation in part (b) and to better observe the region fusion result in part (c).

Our wound boundary determination method is based on three assumptions. First, the foot image contains little irrelevant background information. In reality, it is not a critical problem as we assume that the patients and/or caregivers will observe the foot image with the wound on the camera screen before the image is captured to ensure that the wound is clearly visible. Second, we assume that the healthy skin on the sole of the foot is a nearly uniform color feature. Finally, we assume that the foot ulcer is not located at the edge of the foot outline. These are reasonable assumptions for our initial system development and appear consistent with observations made initially from a small sampling of foot images. In the future, we plan to explore ways to relax these assumptions. [6] discussed about an eye blinking sensor. Nowadays heart attack patients are increasing day by day."Though it is tough to save the heart attack patients, we can increase the statistics of saving the life of patients & the life of others whom they are responsible for. The main design of this project is to track the heart attack of patients who are suffering from any attacks during driving and send them a medical need & thereby to stop the vehicle to ensure that the persons along them are safe from accident. Here, an eye blinking sensor is used to sense the blinking of the eye. spO2 sensor checks the pulse rate of the patient. Both are connected to micro controller. If eye blinking gets stopped then the signal is sent to the controller to make an alarm through the buffer. If spO2 sensor senses a variation in pulse or low oxygen content in blood, it may result in heart failure and therefore the controller stops the motor of the vehicle. Then Tarang F4 transmitter is used to send the vehicle number & the mobile number of the patient to a nearest medical station within 25 km for medical aid. The pulse rate monitored via LCD .The Tarang F4 receiver receives the signal and passes through controller and the number gets displayed in the LCD screen and an alarm is produced through a buzzer as soon the signal is received.

After the foot area is located, we generate a binary image with pixels that are part of the foot labeled "1" (white) and the rest part of the image labeled "0" (black). The result of the foot area determination executed on the region fusion image shown in part (c) in Figure 2 is presented in part (a) in Figure 5. To determine the actual wound boundary, the system locates the black part labeled as "0" within the white foot area (**Hollow region detection in the foot area**). Here we use the simple line-scanning based algorithm illustrated in Figure 4 and explained below.

In this wound boundary determination algorithm, each row in the binary image matrix is regarded as the basic scanning unit. In each row, the part labeled as "0" in the detected foot region is regarded as the wound part. After every row is scanned, the wound boundary is determined accordingly. Because some small outlier regions may also be generated due to the local color variation of the skin, a **Small region filtering** procedure is needed to identify only the largest black region as the wound. A sample of the wound boundary determination result is shown in part (b) in Figure 5.

The RYB (red-yellow-black) wound classification model, proposed in 1988 by Arnqvist, Hellgren and Vincent, is a consistent, simple assessment model to evaluate wounds . It

classifies wound tissues within a wound as red, yellow, black or mixed tissues, which represent the different phases on the continuum of the wound healing process. Specifically, red tissues are viewed as the inflammatory (reaction) phase, proliferation (regeneration), or maturation (remodeling) phase; yellow tissues imply infection or tissue containing slough that are not ready to heal; and black tissues indicate necrotic tissue state, which is not ready to heal either [21] [32]. Based on the RYB wound evaluation model, our wound analysis task is to classify all the pixels within the wound boundary into the RYB color categories and cluster them. Therefore, classical clustering methods can be applied to solve this task.

For our wound image analysis, a fast clustering algorithm called K-mean is applied [22]. K-mean is a simple unsupervised learning algorithm that solves the well-known clustering problem. A sample of the color based wound analysis result is shown in part (c) in Figure 5. The results presented in Section V demonstrate the effectiveness of the K-mean algorithm for our task.

### GPU BASED OPTIMIZATION

Because the CPUs on cameras are not nearly as powerful as those on PCs or laptops, an optimized parallel implementation based on GPUs is critical for the most computationally demanding module in the algorithm structure. For current Android based cameras, such as Nexus 4 from Google, the GPUs (Adreno 320) have high computational capabilities (up to 51.2 G Floating Point Operation per Second (FLOPS)) [33]. As the experimental results in Section V shows, the hybrid implementation on both CPUs and GPUs can significantly improve the time efficiency for algorithms, which are suitable for parallel implementation.

Since our wound analysis is implemented on Android cameras, we take advantage of the Android APIs for GPU implementations. In our case, we use the *Renderscript*, which offers a high performance computation API at the native level written in C (C99 standard) [34] and gives the camera apps the ability to run operations with automatic parallelization across all available processor cores. It also supports different types of processors such as the CPU, GPU or DSP. In addition, a program may access to all of these features without having to write code to support different architectures or a different number of processing cores [35].

### VI. CONCLUSION

We have designed and implemented a novel wound image analysis system for patients with type 2 diabetes suffering from foot ulcers. The wound images are captured by the camera camera placed on an image c wound analysis algorithm is implemented on a camera, utilizing both the CPU and GPU.

We have applied our mean shift based wound boundary determination algorithm to 30 images of moulage wound simulation and additional 34 images of real patients. Analysis of these experimental results shows that this method efficiently provides accurate wound boundary detection results on all wound images with an appropriate parameter setting. Considering that the application is intended for the home environment, we can for each individual patient manually find an optimal parameter setting based on a single sample image taken from the patient before the practical application. Experimental results show that a fixed parameter setting works consistently well for a given patient (same foot and skin condition). In the future, we may consider applying machine learning approaches to enable self-adaptive parameter setting based on different image conditions. The algorithm running time analysis reveals that the fast implementation of the wound image analysis only takes 15 seconds on average on the camera for images with pixel dimensions of 816 x 612.

Accuracy is enhanced by the image capture box, which is designed so that consistent image capture conditions are achieved in terms of the illumination and distance from camera to object. While different camera cameras do have slightly different color space characteristics, we have not included color calibration mainly because the most important aspect of the wound assessment system is the tracking of *changes* to the wound, both in size and color, over consecutive images captures.

Given the high resolution, in terms of pixel size, of all modern camera cameras, the performance of our wound analysis system is not expected to be affected by resolution differences across camera cameras. In fact, the original large resolution images are down-sampled to a fixed spatial resolution of 816 x 612 pixels.

While different image noise levels for different camera cameras is a potential concern, we have determined, based on the experimental results, that any noise level encountered during the image capture process can be effectively removed by applying a Gaussian blurring filter before wound analysis.

The primary application of our wound analysis system is home-based self-management by patients or their caregivers, with the expectation that regular use of the system will reduce both the frequency and the number of wound clinic visits. One concern is that some elderly patients may not be comfortable with operating a camera, but this concern could be addressed by further simplifying the image capture process to a simple voice command.

An alternative deployment strategy is placing the system in wound clinics, where a nurse can perform the wound image capture and data analysis. With this implementation, the wound analysis can be moved from the camera to a server, which will allow more complex and computationally demanding wound boundary detection algorithms to be used. While this will allow easier and more objective wound tracking and may lead to better wound care, this implementation of the wound analysis system is not likely to reduce the number of visits to the wound clinic.

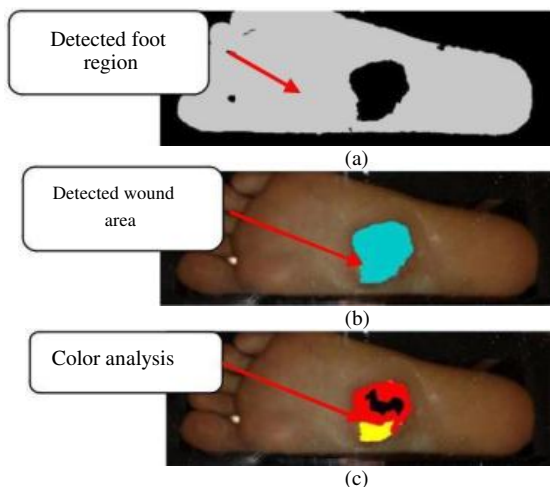


Fig. 5. Wound boundary determination and analysis result. (a) The foot boundary detection result. (b) Wound boundary determination result. (c) Color segmentation result within the wound boundary.

In either implementation, telehealth is an obvious extension to the wound analysis system whereby clinicians can remotely access the wound image and the analysis results. Hence, a database will be constructed on a possibly cloud-based server to store the wound data for patients.

The possibility of microbial contamination of the image capture box by the users or the environment has so far only been addressed by wiping the surface of the box with an antimicrobial wipe after each use. A better solution may be a disposable contamination barrier, which will cover the slanted surface of the box except the openings. This will avoid the patient's foot directly touching the surface of the image capture box.

The entire system is currently being used for wound tracking in the UMass-Memorial Health Center Wound Clinic in Worcester, MA. This testing at the Wound Clinic is a first step toward usability testing of the system by patients in their homes.

In future work, we plan to apply machine learning methods to train the wound analysis system based on clinical input and hopefully thereby achieve better boundary determination results with less restrictive assumptions. Furthermore, we plan to compute a healing score to be assigned to each wound image to support trend analysis of a wound's healing status.

#### ACKNOWLEDGEMENT

The authors would like to thank all the reviewers for their constructive comments which greatly improve the scientific quality of the manuscript.

#### VII REFERENCES

- [1] K.M. Buckley, L.K. Adelson and J.G. Agazio, "Reducing the risks of wound consultation: Adding digital images to verbal reports," *Wound Ostomy Continence Nurs.*, vol. 36, no. 2, pp. 163-170, Mar. 2009.
- [2] V. Falanga, "The chronic wound: Impaired healing and solutions in the context of wound bed preparation," *Blood Cells Mol. Dis.*, vol. 32, no. 1; pp. 88-94, Jan. 2004.
- [3] C.T. Hess and R.S. Kirsner, "Orchestrating wound healing: Assessing and preparing the wound bed," *J. Adv. Skin Wound Care*, vol. 16, no. 5, pp. 246-257, Sep. 2006.
- [4] R.S. Rees and N. Bashshur, "The effects of Tele wound management on use of service and financial outcomes," *Telemed. J. E. Health*, vol. 13, no. 6, pp. 663-674, Dec. 2007.
- [5] National Institute of Health. "NIH's National Diabetes Information Clearing House," [Online], Available from: [www.diabetes.niddk.nih.gov](http://www.diabetes.niddk.nih.gov).
- [6] Christo Ananth, S.Shafiq Shalaysha, M.Vaishnavi, J.Sasi Rabiyaathul Sabena, A.P.L.Sangeetha, M.Santhi, "Realtime Monitoring Of Cardiac Patients At Distance Using Tarang Communication", *International Journal of Innovative Research in Engineering & Science (IJRES)*, Volume 9, Issue 3, September 2014, pp-15-20
- [7] H. Wannous, Y. Lucas, S. Treuillet, B. Albouy, "A complete 3D wound assessment tool for accurate tissue classification and measurement," *IEEE 15<sup>th</sup> Conf. on Image Processing*, pp. 2928-2931, Oct. 2008.
- [8] P.Plassman, T.D. Jones, "MAVIS: A non-invasive instrument to measure area and volume of wounds," *Med. Eng. Phys.*, vol. 20, no. 5, pp. 332-338, Jul. 1998.
- [9] A. Malian, A. Azizi, F.A. Van den Heuvel, M. Zolfaghari, "Development of a robust photogrammetric metrology system for monitoring the healing of bedsores," *Photogrammetric Record*, vol. 20, no.111, pp. 241-273, Jan. 2005.